

Investigating the pattern transfer fidelity of Norland Optical Adhesive 81 for nanogrooves by microtransfer molding

Cite as: J. Vac. Sci. Technol. B **39**, 062810 (2021); <https://doi.org/10.1116/6.0001333>

Submitted: 04 August 2021 • Accepted: 11 November 2021 • Published Online: 02 December 2021

 Rahman Sabahi-Kaviani and  Regina Luttgé

COLLECTIONS

Paper published as part of the special topic on [64th International Conference on Electron, Ion, And Photon Beam Technology and Nanofabrication, EIPBN 2021](#)



View Online



Export Citation



CrossMark

ARTICLES YOU MAY BE INTERESTED IN

[Biological tissues as mechanical metamaterials](#)

Physics Today **74**, 30 (2021); <https://doi.org/10.1063/PT.3.4900>

[Exploring liquid plasma jets using short laser pulses](#)

Scilight **2021**, 491110 (2021); <https://doi.org/10.1063/10.0008947>

[Sketch graphs](#)

The Physics Teacher **59**, 675 (2021); <https://doi.org/10.1119/10.0007370>



Advance your science and
career as a member of

AVS

LEARN MORE



Investigating the pattern transfer fidelity of Norland Optical Adhesive 81 for nanogrooves by microtransfer molding

Cite as: J. Vac. Sci. Technol. B 39, 062810 (2021); doi: 10.1116/6.0001333

Submitted: 4 August 2021 · Accepted: 11 November 2021 ·

Published Online: 2 December 2021



Rahman Sabahi-Kaviani and Regina Luttgé ^{a)}

AFFILIATIONS

Neuro-Nanoscale Engineering, Department of Mechanical Engineering/Microsystems and Institute of Complex Molecular Systems, Eindhoven University of Technology, 5600MB Eindhoven, The Netherlands

Note: This paper is part of the Special Collection: 64th International Conference on Electron, Ion, And Photon Beam Technology and Nanofabrication, EIPBN 2021.

^{a)} Author to whom correspondence should be addressed: r.luttge@tue.nl

ABSTRACT

We demonstrated the microtransfer molding of Norland Optical Adhesive 81 (NOA81) thin films. NOA81 nanogrooves and flat thin films were transferred from a flexible polydimethylsiloxane (PDMS) working mold. In the case of nanogrooves, the mold's feature area of $15 \times 15 \text{ mm}^2$ contains a variety of pattern dimensions in a set of smaller nanogroove fields of a few mm^2 each. We demonstrated that at least six microtransfers can be performed from the same PDMS working mold. Within the restriction of our atomic force microscopy measurement technique, nanogroove height varies with $82 \pm 11 \text{ nm}$ depending on the pattern dimensions of the measured fields. Respective micrographs of two of these fields, i.e., one field designated with narrower grooves (D1000L780, case 1) and the other designated with wider grooves (D1000L230, case 2) but with the same periodicity values, demonstrate faithful transfer of the patterns. The designated pattern dimensions refer to the periodicity (D) and the ridge width (L) in the original design process of the master mold (dimensional units are nm). In addition, neither NOA81 itself (flat films) nor NOA81 nanogroove thin films with a thickness of $1.6 \mu\text{m}$ deteriorate the imaging quality in optical cell microscopy.

© 2021 Author(s). All article content, except where otherwise noted, is licensed under a Creative Commons Attribution (CC BY) license (<http://creativecommons.org/licenses/by/4.0/>). <https://doi.org/10.1116/6.0001333>

I. INTRODUCTION

To be able to further our knowledge on nanogroove-cell interactions with different materials, we investigate in this paper the fabrication method of Norland Optical Adhesive 81 (NOA81) nanogrooves by microtransfer molding.

NOA81 (Norland Products Inc., NJ, USA) is a single component adhesive which is applied in liquid form and subsequently cured under ultraviolet (UV) light within a few seconds to minutes at a peak sensitivity around a wavelength of 365 nm .¹ This transparent material was first introduced as a fast bonding agent for optical components and later as a biocompatible alternative for polydimethylsiloxane (PDMS) in microfluidics,² cost-effective micro-channel fabrication,³ and cell culture devices,^{4,5} including brain-on-chip (BOC) applications.^{6,7} Microfluidic BOCs have

emerged rapidly in the BioMEMS field to advance neurodegenerative disease modeling.^{8–10} Furthermore, the toolbox for clinical relevant organ and disease models relies on innovative micro- and nanofabrication techniques, allowing the mimicry of well-defined, reproducible, and controllable microenvironments for culturing tissues.^{11–15} These *in vivo* like environments can be designed to exert control over the organization, manipulation, and analysis of the cultured cells. In particular, topographical features and material stiffness affect cells' morphology during the neuronal cell network formation *in vitro*.^{16–21} Hence, in culturing neuronal cells, nanoscale topographies can alter neural cell network architecture, enhancing neuronal differentiation and, therefore, advance *in vitro* neurodegenerative disease models.

In our previous work, we demonstrated nanogrooves made of silicon nanoimprint resist as well as PDMS of which the latter

showed at different ratios of elastomer and curing agent alterations in soma size and neural outgrowths.²¹ In another effort, we also demonstrated the feasibility of nanogroove replica molding in Ostermer.²² Compared to these materials, NOA81 has a higher Young's modulus (1.38 GPa)²³ than PDMS (0.57–3.7 MPa depending on the elastomer base to curing agent ratio of 33:1 to 5:1)²⁴ but has a similar high Young's modulus as commercially available Ostermer (OSTEMER 322 Crystal Clear, Mercene Labs, Stockholm, Sweden).^{25,26} In addition, NOA81 showed good cell compatibility, optical performance, and mechanical stability in microsieve-assisted cell cultures.⁶ Moreover, NOA81 demonstrated to be a useful mold material for the production of large aspect ratio structures even with the nanoscale size.²⁷ Benefitting from our experience in expanding pattern fidelity in the fabrication process of NOA81 microsieves,⁷ we hypothesize that the material can further add to the *in vitro* organ-on-chip and disease modeling toolbox. Therefore, we proposed here the application of microtransfer molding as a new fabrication method for NOA81 nanogroove thin films.

Microtransfer molding (μ TM) is known as a variation of soft lithography to assemble a wide range of micro- and nanopatterned materials in 2D/3D spatially organized platforms.²⁸ Creating reproducible patterns with well-defined layer thickness is critical, especially in microscopic observations of cells, as any variation in the patterns and thickness of the film might influence the cells' behavior and the outcome of the image quality. Not only film thickness variations and substrate uniformity but also optical path length and its variations through the material stacks of the devices used in optical imaging of cells should be kept minimal for high optical performance. Hence, the control of the film's thickness below a couple of micrometers is essential. On the other hand, handling a very thin NOA81 foil is almost impossible; therefore, here the aim is to solve this handling challenge by microtransfer of a spin-coated NOA81 thin film to an acceptor substrate. We further demonstrate the integration of NOA81 nanogroove thin films in a well-plate format for biological experiments.

II. EXPERIMENT

A. Nanogroove fabrication

1. PDMS working mold

A cyclic olefin copolymer (COC) nanogroove master mold for fabrication of PDMS working molds was used in these experiments. This mold was previously fabricated utilizing jet-and-flash imprint lithography (J-FIL) and thermal nanoimprint lithography by Xie.²⁹ A detailed description of the PDMS working mold fabrication steps was given already by Xie and Lutge³⁰ and Bastiaens *et al.*²² To recap, fabrication of a nanoresist scaffold on a silicon wafer is realized by means of pattern transfer from an originally manufactured quartz stamp using electron beam lithography and etching. The stamp contains 27 fields with nanogrooves of a variety of dimensions. Resolved pattern periodicity (D) ranged from 200 to 2000 nm with ridge widths (L) from 100 to 1340 nm, and a resist height of 118 nm in the original jet-and-flash nanolithography step. Next, the patterns on the fabricated nanoresist scaffold were transferred into a COC substrate (optical grade TOPAS 8007S-04,

Kunststoff-Zentrum) by a thermal nanoimprint lithography system (EITRE 6, Obducat) at a temperature of 108 °C while a pressure of 4 MPa was applied. The COC [Fig. 1(i)] is subsequently used to fabricate the PDMS working mold for this research on NOA81 nanogroove thin-film microtransfer molding.

The PDMS working mold is hence an inverted copy of the patterns in the COC master mold and was fabricated using PDMS elastomer and cross-linking agents (SYLGARD 184, Dow Corning, Midland, MI, USA) mixed at a ratio of 10:1. The mixture was first degassed for 20 min in a vacuum desiccator. Subsequently, PDMS was poured on the COC master mold and spin-coated (WS-650Series Spin Processor, Laurell Technologies, PA, USA) for 30 s with 250 rpm to achieve an $\sim 200\ \mu\text{m}$ thick PDMS layer [Fig. 1(ii)]. After placing the assembly in an oven at 65 °C for 2 h, the completely cured PDMS was peeled off from the COC. Next, a set of nanogrooved fields of interest were cut by a scalpel to size (here, $15 \times 15\ \text{mm}^2$) and was then carefully placed by a fine tweezer on a clean cover glass (Thermo Scientific, Menzel-Gläser, Germany) with a diameter of 30 mm with the nanogroove features facing up for further handling steps during fabrication.

2. Microtransfer molding

To allow the wetting of NOA81 during spin-coating, the PDMS working mold surface needs to be hydrophilic. Therefore, it was treated with oxygen plasma for 30 s with 3 W in a plasma asher (EMITECH K1050X, Quorum, Laughton, UK) [Fig. 1(iii)]. The surface of the PDMS working mold has been shown to remain activated throughout six consecutive microtransfer molding steps. Shortly after this surface activation, the NOA81 liquid was poured in excess on the PDMS mold [Fig. 1(iv)] and spin-coated in three successive spinning steps: starting with (a) 500 rpm for 30 s at an acceleration of 200 rpm/s, then continue spinning (b) for 60 s at a speed depending on the desired final NOA81 film thickness with an acceleration of 500 rpm/s, and finally (c) decelerating at 1000 rpm/s [Fig. 1(v)]. Finally, the NOA81 nanogroove thin film is ready for the microtransfer molding step onto the surface of an acceptor substrate.

To demonstrate microtransfer molding of the NOA81 nanogroove thin film, the NOA81-loaded PDMS mold was peeled off from the coverslip and flipped over onto the acceptor substrate, here a glass slide (VWR, Catalog Number 631-1552, The Netherlands). Positioning of the mold onto the acceptor substrate is performed by starting from one corner of the mold with caution in order to avoid trapping any air bubbles between the film and the glass. After this step, the stack was placed inside a UV-LED exposure system (IDONUS, UV-EXP 150R, Neuchatel, Switzerland) to receive a light dose of $4000\ \text{mJ}/\text{cm}^2$ with the intensity set to $15\ \text{mW}/\text{cm}^2$ [Fig. 1(vi)]. The mold was then peeled off from the precured NOA81 and the microtransferred patterned film received an additional light dose of $5000\ \text{mJ}/\text{cm}^2$ with the same intensity settings to fully cure the NOA81 nanogroove thin film on the glass substrate [Fig. 1(vii)]. Additionally, we examined the possibility of microtransfer molding of an NOA81 nanogroove thin film to other acceptor substrates, e.g., on a flat NOA81, too. To create a flat NOA81 substrate, liquid NOA81 was poured on a coverslip and spin-coated at 800 rpm for 60 s. Subsequently, it was placed

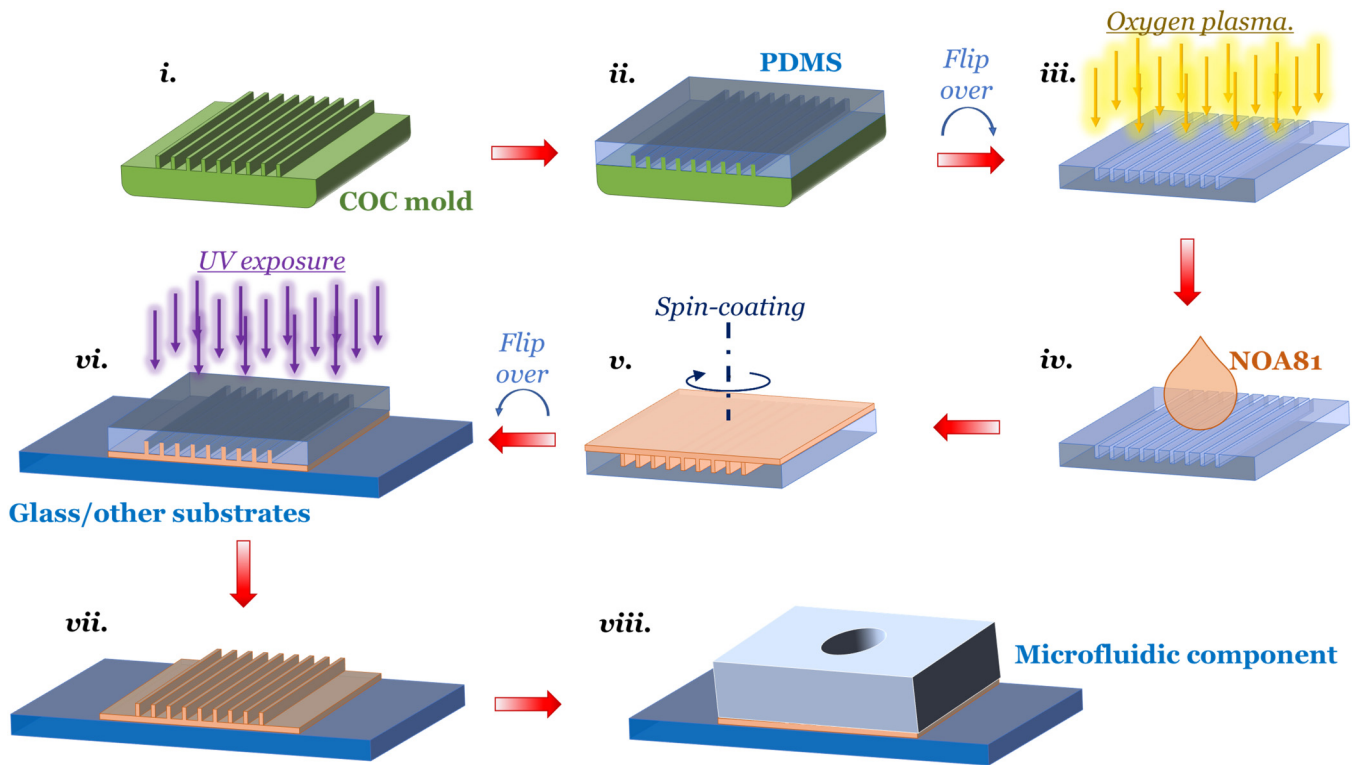


FIG. 1. Schematic representation of the steps of the new fabrication method: (i) access to a master, here containing an area of a set of 27 smaller nanogroove fields in COC, each with an area of $\sim 3 \times 9 \text{ mm}^2$; (ii) replication of nanogrooves from the COC master to a PDMS working mold; (iii) oxygen plasma treatment of the working mold to yield a hydrophilic surface; (iv) dispensing NOA81 liquid on the PDMS working mold; (v) spin-coat NOA81 on to the mold; (vi) microtransfer molding of NOA81 nanogroove thin film on to an acceptor substrate and exposure under UV light through UV transparent PDMS mold to semicure NOA81; (vii) peeling off the PDMS mold from the transferred NOA81 nanogroove thin film and perform an additional UV exposure to fully cure NOA81 on the acceptor substrate; and (viii) assembly with other components.

under a UV-LED exposure system to receive energy dosage of 9000 mJ/cm^2 , with the above-mentioned intensity settings.

B. Characterization of the nanogroove dimensions in the PDMS working mold and of the corresponding NOA81 nanogroove thin films

To measure the thickness of a transferred NOA81 thin film on the acceptor substrate, the samples were submitted to a Dektak XT profilometer (Bruker Corporation, MI, USA). The nanogrooves in the PDMS working mold and the microtransfer molded NOA81 nanogroove thin film patterns were examined by scanning electron microscopy (SEM). The SEM images of two selected patterned fields (case 1 and 2) were taken using a QUANTA 600F tool (FEI, The Netherlands) in the low vacuum mode. Additionally, surface topographies of the transferred NOA81 nanogrooves were studied in more detail by applying atomic force microscopy (AFM). Topographical data from the samples were acquired and recorded by XE-100 (Park Systems Corporate, Suwon, Korea) in the tapping mode and with a noncontact cantilever (PPP-NCHR, Park Systems Corporate, Suwon, Korea). This AFM tool runs in the XEP software (Park Systems

Corporate, Suwon, Korea). However, to analyze the captured data, GWYDDION software³¹ is used. For a simple and quick optical performance test of microtransferred NOA81 flat or nanogroove thin films on glass substrates, these were mounted underneath of a culture dish containing differentiated neural stem cells, and respective images were taken using a Leica DMI8 fluorescent microscope (Leica Microsystems, Wetzlar, Germany) in the phase contrast mode.

C. Fabrication of a well-plate

To provide a single well-plate implementing nanogrooves, e.g., neural cell culture platforms, a flat PDMS slab with a thickness of 3 mm is fabricated and cut to $15 \times 15 \text{ cm}^2$ pieces [Fig. 1(viii)]. These pieces were punched in the center using a 3 mm diameter biopsy puncher. Such a simple PMDS reservoir was also fabricated using the PDMS mixing, degassing, and curing protocols described in Sec. II A 1 and pouring the mixture on a clean silicon wafer, which was precoated with the silanization agent 1H, 1H, 2H, 2H-perfluorodecyl-triethoxysilane (658758, Sigma Aldrich, Zwijndrecht, The Netherlands) for 2 h inside a vacuum desiccator. To adhere NOA81 nanogrooves to the PDMS slabs, we

used an additional amount of NOA81 liquid as bonding agent. For this purpose, the bottom side of the PDMS slab was treated with oxygen plasma for 30 s with 3 W to provide the wetting properties of the surface. Then, several NOA81 drops were transferred carefully using a sharp tip onto the PDMS part evenly distributed on the surface around the punched hole. Next, the hole in the PDMS slab was manually positioned to the desired location on the NOA81 nanogroove thin films and subsequently exposed to UV light to complete the assembly and bonding process between the parts using the settings previously mentioned in Sec. II A 2. To verify whether the bonding process between the PDMS and NOA81 parts provides a leak-free device, a dye solution contacting Brilliant Black BN (Sigma Aldrich, Germany) dissolved in deionized water (1 mg/ml) was prepared and added in the reservoir.

III. RESULTS AND DISCUSSION

A. NOA81 nanogrooves

Although the details of nanoscale-size patterns are not visible by the naked eyes, all patterned fields are still resulting in

groovelike features discernible by the interference effect of these grating structures. Although the high quality in transferring the smallest features by jet-and-flash nanoimprint lithography from the original quartz stamp into nanoresist scaffolds has been jeopardized by applying multiple copies in the process to reach the final NOA81 nanogroove thin films on acceptor substrates, microtransfer molding is successfully demonstrated according to the description given in Sec. II A. The presence of nanogrooves in the PDMS working mold [Fig. 2(a)] as well as successful transfer molded NOA81 nanogroove thin films on glass [Fig. 2(b)] and flat NOA81 [Fig. 2(c)] acceptor substrates can be already confirmed by the appearing colors due to light interference in normal room light. The thickness of the PDMS working mold and the microtransferred NOA81 nanogroove thin film is ~ 200 and $1.6 \mu\text{m}$, respectively. In the experiments, a working mold with an area of $\sim 15 \times 15 \text{ mm}^2$ is demonstrated containing fewer variations of nanogroove patterns, which, for the purpose of this experiment, was simply cut manually from the larger PDMS replica containing the full array of all 27 patterned fields using a scalpel. For a more detail visualization of the microtransfer results of these anisotropic nanotopographic features

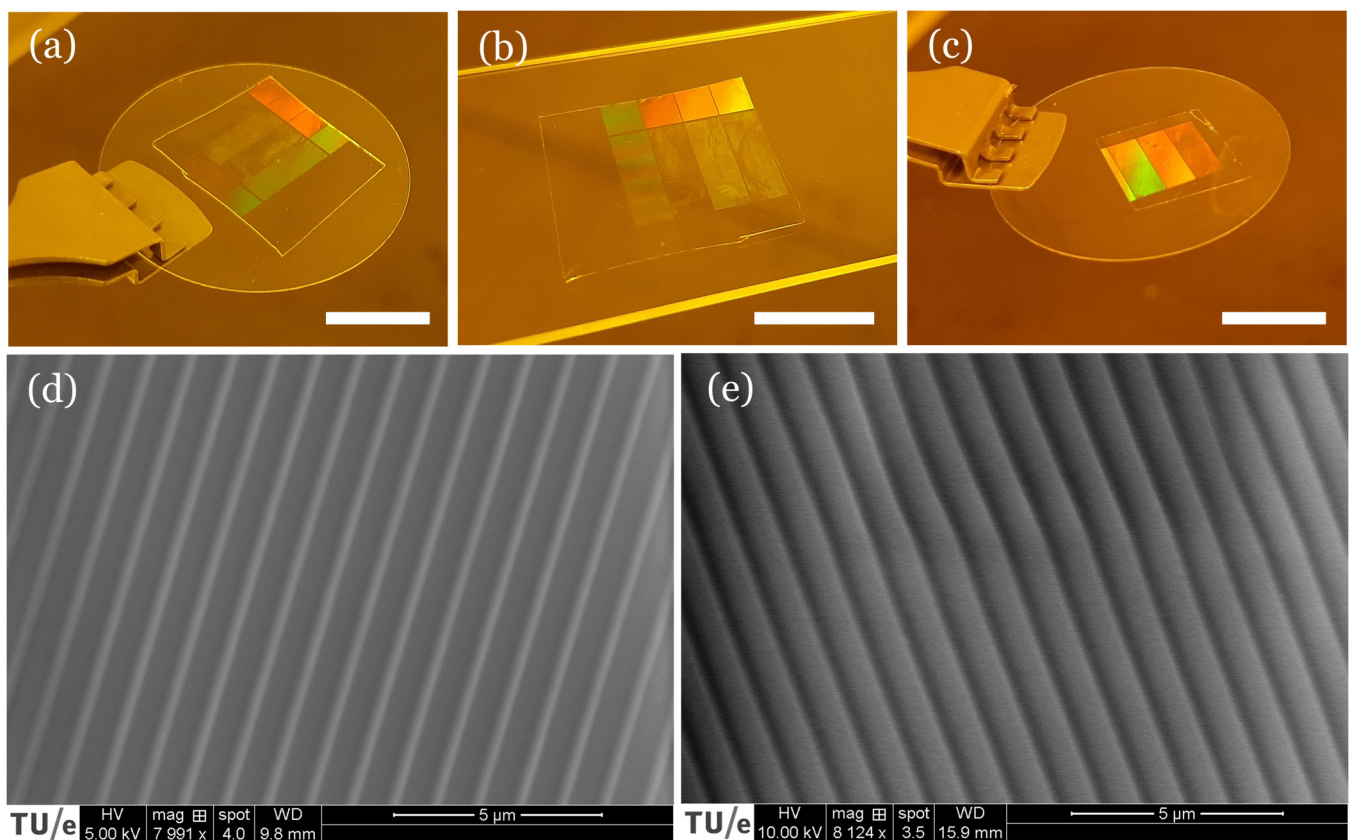


FIG. 2. Nanogroove patterns are visible by appearing colors due to light interference on the surface of the PDMS working mold (a), and after the transfer of NOA81 thin films onto a microscope glass slide (b) as well as onto the flat NOA81 that was spin-coated and cured on the coverslip acceptor substrate prior to the NOA81 microtransfer molding step (c). SEM images show the microtransferred NOA81 nanogroove thin film onto a glass substrate for the two types of selected pattern cases 1 and 2, D1000L780 (d) and D1000L230 (e), respectively. Scale bars: 1 cm for (a)–(c).

on the substrate, an NOA81 nanogroove thin film on a glass slide was observed by SEM. For this purpose, two SEM samples were prepared, one sample was marked-up in the COC mold having a nanogroove pattern periodicity (D) of 1000 and a ridge width (L) marked-up as 780 (here, referred to as case 1: D1000L780), and the other having a nanogroove pattern periodicity (D) of also 1000 but a ridge width (L) of 230 (here, referred to as case 2: D1000L230). As can be observed from these two SEM images, microtransfer molding using PDMS molds for case 1 [Fig. 2(d)] has a good visibility of the groove bottom due to the lower filling factor compared to the resulting nanogrooves in case 2, in which the bottom of the grooves is harder to be visualized [Fig. 2(e)]. The SEM micrographs taken for these two patterns qualitatively confirm the presence of nanogrooves in NOA81 after microtransfer molding. However, more accurate measurements were obtained by atomic force microscopy and the results thereof are discussed in Sec. III B.

B. Nanogroove pattern transfer fidelity

To assess the pattern transfer performance of NOA81 nanogrooves by microtransfer molding in a quantitative manner, AFM area plots of the PDMS working mold structure and their resulting NOA81 relief pattern on glass substrates were recorded. For this purpose, like in the SEM images, the two PDMS working mold patterns marked-up with D1000L780 and D1000L230 were examined

by means of an example for the pattern fidelity. After transfer molding NOA81 nanogroove thin films, the patterned fields marked-up with the same description were then scanned by AFM. The fabricated nanogroove periodicity can also be experienced in an optical diffraction experiment, which is elaborated in the supplementary material.⁴² In AFM, an area of $6 \times 6 \mu\text{m}^2$ on all the surfaces have been explored, and the measurement resolution was set to 256×256 pixels. Figures 3(a) and 3(b) present the nanogroove topography recognized in the PDMS mold and NOA81 transferred on glass substrate, with the PDMS mold having pattern parameters of D1000L780. Accordingly, Figs. 3(c) and 3(d) show the topographies on the PDMS mold and NOA81 thin films for case 2, i.e., D1000L230. Figures 3(e) and 3(f) depict the line profiles between the PDMS working molds against the ones of the transferred NOA81 nanogroove thin film, for D1000L780 and D1000L230, respectively. In these two figures, the transferred NOA81 nanogrooves have the inverse shape; yet, similar pattern line profiles are clearly recognized. In more details, in the case of using mold features designated D1000L780, the nanogrooves of PDMS have a measured periodicity of $951.0 \pm 8.0 \text{ nm}$ and a ridge height of $71.9 \pm 4.1 \text{ nm}$ ($n = 4$), while for the transferred NOA81 nanogrooves, the inverted pattern has a periodicity of $980.5 \pm 6.5 \text{ nm}$ and a ridge height of $68.9 \pm 1.1 \text{ nm}$ ($n = 4$). Here, “n” refers to the number of consecutive groove features on the same profile line. The analysis for the second case (the patterned field marked with

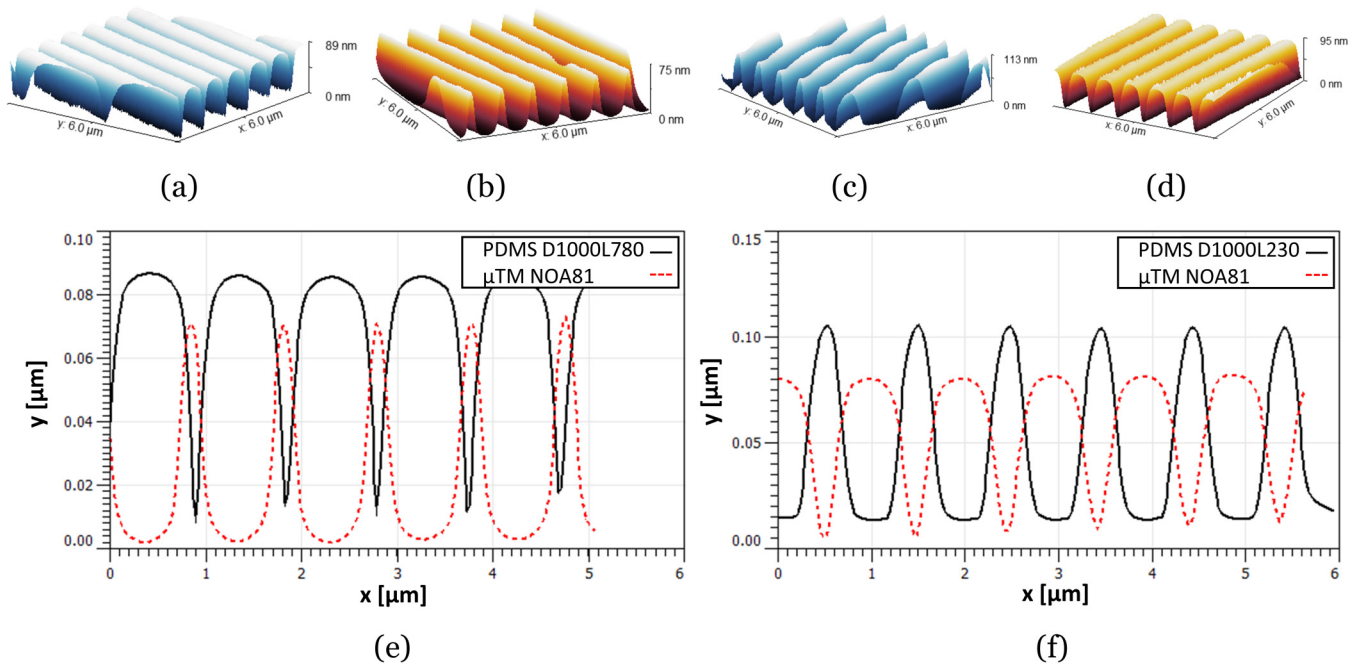


FIG. 3. AFM is used to measure nanogroove patterns on the PDMS working mold and their corresponding microtransfer molded NOA81 nanogroove thin film on glass substrates. These AFM data are depicted as 3D topographic area plots for PDMS with nanogroove pattern periodicity of 1000 nm and ridge width of 780 nm (D1000L780, case 1) (a) and its resulting transferred NOA81 nanogrooves (b), as well as for PDMS with nanogroove pattern periodicity of 1000 nm and ridge width of 230 nm (D1000L230, case 2) (c) and the resulting transferred NOA81 nanogrooves using this mold (d). Moreover, the respective cross-sectional line profiles are presented for the same designated pattern parameters, i.e., D1000L780 (e) and D1000L230 (f).

D1000L230) has a measured periodicity of 979.0 ± 8.0 nm and a ridge height of 91.3 ± 0.7 nm ($n = 4$) for the PDMS mold and periodicity of 971.0 ± 0.5 nm and ridge height of 78.1 ± 1.8 nm ($n = 4$) for the NOA81 transfer. The results show that by using microtransfer molding, these nanoscale-sized structures can be transferred from PDMS working molds within reasonable error margins. Although the change in the nanogroove height could potentially be an influential factor in the cell experiments, since the height affects cell culture results, nanogroove dimensions within the range of the measured values from the structures gained in this work have expressed an alignment effect on neuronal cell growth.³² Even though in the first case (D1000L780) we did not observe a substantial difference in the measured nanogroove height, a reduction by $\sim 24\%$ was detected for the second case (D1000L230). However, the overall reduction in height in either case is not significant and since the values are measured from a random spot on the surfaces and not the same location, the achieved fluctuation might result from this random factor. Moreover, the reported data are the average of four consecutive groove features on the same profile line, and that is also limiting the final measurement. To address the potential causes of a change in height, we can mention the restriction in the resolution of the AFM measurements due to the size of the AFM cantilever probe tip. Moreover, the narrow width of the grooves could also lead to the incomplete release of NOA81 during the microtransfer step, although in the present study we did not find evidence for such a defect. Another potential cause of change in height of the final NOA81 ridges compared to the original grooves in the COC master mold could be related to the PDMS mold, where in the PDMS mold grooves were not fully filled with NOA81, or during the PDMS working mold fabrication the narrower the nanogrooves in the COC, the lesser the likelihood that these structures were equally filled with PDMS initially. Hence, we refer to the PDMS working mold as a reference for performance evaluation of the NOA81 pattern transfer fidelity rather than the original COC mold. By increasing the resting time of the filling material into a mold³³ (as for NOA81 on PDMS as a filling material) before transfer or release or by applying additional treatments to the mold surface, like surface modifying coatings beyond a simple oxygen plasma,^{34,35} filling and release properties can be facilitated and hence could also result in further improvements of the pattern fidelity for such narrow features. Finally, although the dimensions of the microtransfer molded NOA81 nanogroove thin film were measured on glass substrates, we did not expect that the acceptor substrate material influenced the pattern transfer fidelity directly, but it may influence the measurement results in AFM since such a glass carrier substrate is a stiff substrate and the NOA81 film is relatively thin. Overall, the results on the transfer performance itself can be probably generalized for other acceptor substrate materials as long as the adhesion of the precured NOA81 to the acceptor substrate material is higher than the adhesion to the PDMS working mold and the carrier substrate is not a soft substrate.

Based on AFM data, the measured microtransfer molded features demonstrate a good pattern transfer fidelity between the PDMS mold and the released NOA81 nanogroove thin films. However, it is essential to study the pattern transfer process in more detail also using scanning electron microscopy in characterizing also the cross-sectional shape and evaluating also the bottom of

the nanogroove features carefully prior to utilizing such patterns in cell culture experiments. Here, to provide an insight into the sidewalls of the nanogrooves as shown in Fig. 4, an SEM image was taken under the condition when the sample was tilted by 30° (see Fig. S2 in the supplementary material).⁴² If the patterns are faithfully transferred indeed, this route of fabrication could add value by economically attractive multiplying such cell culture substrates in sufficient high numbers from the same mold. Hence, we also investigate whether the described fabrication process deteriorates the patterns and damages the nanogroove on the PDMS working mold after multiple microtransfer molding steps from the same mold. To be able to characterize the process on this merit, a PDMS mold with nanogroove patterns of D1000L780 was selected, and this specific PDMS mold was used six consecutive times to produce multiples of the NOA81 nanogroove thin-film topology. The PDMS mold was fabricated with a thickness of $\sim 200 \mu\text{m}$; hence, its flexibility granted a high control over performing the transfer step compared to the situation when a thicker PDMS mold was applied. Using thicker molds hampered handling and led to air bubble entrapment. Therefore, to have a higher process capability in microtransfer molding, we keep the mold relatively thin; however, if it is too thin (e.g., $100 \mu\text{m}$), the mold ruptured after the second transfer. While this may be fixed with a stronger backing plate attached to the mold after transfer but prior to peeling the mold off the transferred film, we successfully demonstrated here that a $200\text{-}\mu\text{m}$ PDMS mold suffices and six consecutive NOA81 nanogroove microtransfers were performed. By means of an example of all the line profiles taken from the six NOA81 transferred thin films (see additional data shown in S1 in the supplementary

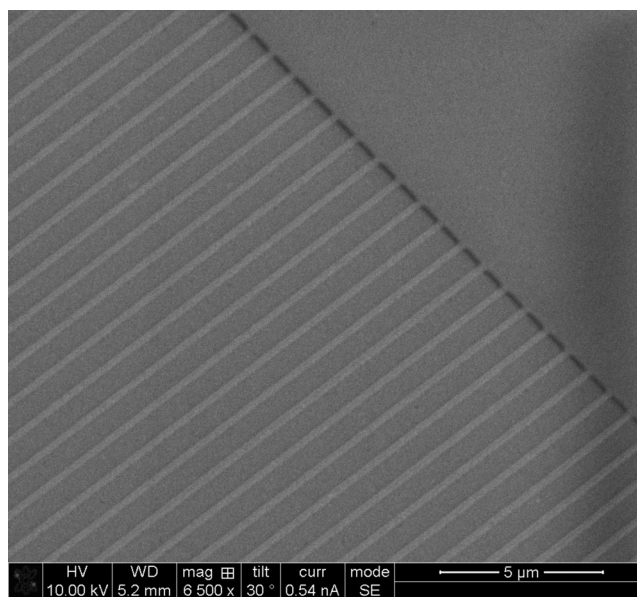


FIG. 4. SEM image of the microtransfer molded NOA81 nanogroove that was tilted with 30 degrees to provide an insight into the sidewalls of the nanogrooves (~ 20 nm of gold was sputtered on the sample prior to SEM imaging).

material),⁴² the AFM results of the first and the sixth transfer are depicted in Fig. 5 next to the equivalent line scan of respective pattern in the PDMS working mold. Furthermore, the data in Fig. 5 show that the first transfer has patterns with a periodicity of 980.5 ± 6.5 nm with a ridge width of 232.5 ± 1.5 nm and a ridge height of 68.9 ± 1.1 nm ($n=4$). Here, the ridge width is measured at half height of the received signal and “n” refers to the number of consecutive groove features on the same profile line. The parameters for the sixth transferred NOA81 nanogrooves with the same mold are 980.5 ± 19.5 nm for the pattern periodicity, 261.0 ± 5.0 nm for ridge width, and 79.8 ± 2.2 nm for the ridge height ($n=4$). As shown in Fig. 5, the two profiles are well-matched, and the ridge width did not change substantially. In conclusion, it is shown that the successful repetition of the microtransfer molding step from the same PDMS working mold to NOA81 nanogrooved thin films including a plasma process and consecutive repetition of peeling off precured NOA81 can be realized.

Consequently, if one wanted to move from simple research substrates in biology to the manufacturing of robust brain-on-chips, the whole fabrication chain should be validated. Hence, the influence of the various parameters per step in the complete fabrication procedure starting with the master mold should be discussed thoroughly. To this end, we can contribute as follows.

An enduring master mold is important for the repeatability of this fabrication method in production across multiple batches of PDMS working molds. The proposed method uses a COC master mold, which has been devised as a more durable master mold for the PDMS replication by soft lithography than a simple nanoresist on silicon master mold, which was made by step-and-flash nanolithography.²⁹ This COC master mold was fabricated several years ago and is still used for experiments today to fabricate PDMS replicas thereof, which are here used as the working molds for the NOA81 microtransfer printing process.

The thermally nanoimprinted COC may have faced material aging, and the structural dimensions of COC mold could be

affected by various temperature processes. In all our processes, we aimed to keep the temperature at 65°C or below to cure the PDMS, and it does not exceed the glass transition temperature (T_g) of COC (78°C); hence, the patterns are preserved accordingly. Multiple uses of this mold over years for replication of several PDMS parts, however, can cause damage to the ridges by scratches and the geometry of the ridge and groove pattern may have been affected by accidentally heating the COC master above T_g leading to reflow. This effect would then potentially decrease the structural height by transition of the rectangular ridge to a more semicircular cross-sectional shape, but if this occurred most likely, we should see this also in a change of the pattern periodicity. AFM does not show any significant change in periodicity compared to the originally designed periodicity, neither in the simple diffraction test that is given in the supplementary material.⁴² Hence, we can conclude that if such damage would have occurred, it is very small.

More importantly, the PDMS working mold is a part that wears during (1) plasma treatment and (2) release of the NOA81 film after transfer. The PDMS used here is prepared using the base elastomer and cross-linking agents mixed at a ratio of 10:1 demonstrated up to six consecutive replicas without significant damage, yet. Changing the mixing ratio differs the material properties of the PDMS working mold such as density,³⁶ stiffness,³⁷ viscosity, and ultimate tensile stress.³⁸ Since the replication of the PDMS part employs a spin-coating step at a certain spinning speed on the COC mold, a change in the viscosity of the PDMS mix will influence the PDMS mold thickness. The latter can have an influence on the microtransfer performance, which should be investigated in greater detail for setting up a production process. PDMS of a higher viscosity might also need a longer resting time for the PDMS to fully fill the grooves in the COC, which can also have an influence on the cross-sectional shape that is finally transferred into the NOA81, and batch to batch variations on the shape could occur. This is more critical for the patterns on the COC master mold with very small dimensions to be transferred. A detailed study into the actual critical dimensions of this process is still required to give a more conclusive answer. However, given the fact that PDMS soft lithography has been recognized as a high-resolution lithography technique, it is probably (after some level of optimization) not a concern for the nanogrooves envisaged in BOC, which aims for a 400–2000 nm periodicity. The repetitive use of the PDMS working mold during transfer printing could affect some properties of the cured PDMS, too. For example, it increases Young’s modulus over time meaning the molds become stiffer gradually.³⁹ Therefore, for using the molds that are stored for a long time, this factor needs to be explored comprehensively to address the repeatability of the process in manufacturing.

In the spin-coating step, spin speed is a factor that controls the thickness of the mold directly and is an influential feature in the transfer step. This was touched upon earlier in this section. However, most influential for a properly spin-coated layer of NOA81 on the PDMS working mold is its surface property. Prior to spin-coating of NOA81, PDMS is exposed to an oxygen plasma, whereas power and time provide the main parameters of the process window in this step. This treatment makes the PDMS surface hydrophilic. NOA81 will spread more uniformly on a hydrophilic mold during the spin-coating step. However, this

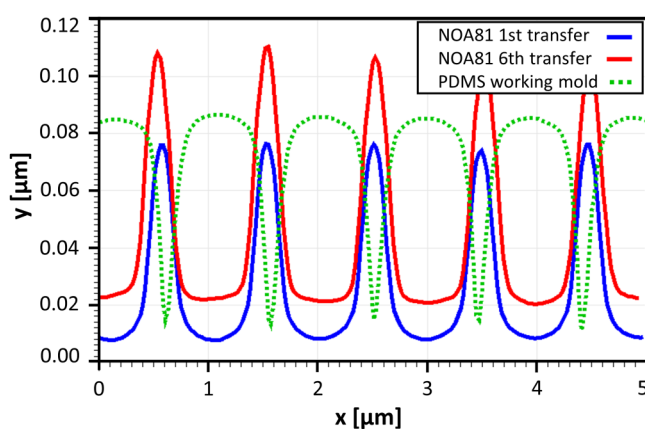


FIG. 5. Cross-sectional line profiles by AFM for consecutive transfers made using the same PDMS mold with pattern parameters of case 1 (D1000L780) and line profile across the nanogrooves of the mold.

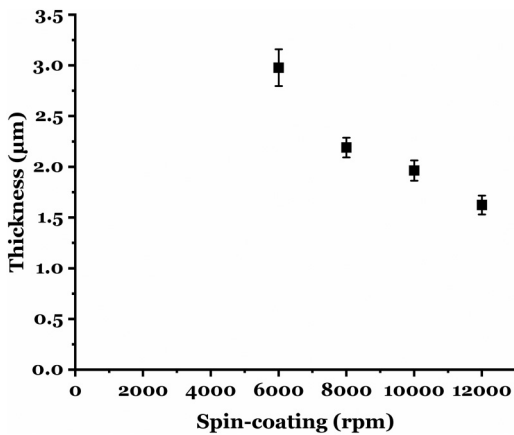


FIG. 6. NOA81 microtransfer molded film thickness on a glass substrate for different spin-coating speeds.

surface is thermodynamically unstable and loses its hydrophilic property and becomes again hydrophobic in an hour due to low molecular weight chains that over time diffuses to the surface.^{40,41} It has been observed in our experiments that when NOA81 is cured on a nonmodified PDMS mold, the cured NOA81 can be easily peeled off but wetting is not as good as in the case of improved wettability after repetitive plasma treatments just prior to the spin-coating step. Unfortunately, with these repetitive plasma treatments, NOA81 gets gradually more difficult to be peeled off. Still, these conflicting requirements for wetting/peeling within the current process window yield at least six repetitions. Here, overall the plasma asher properties such as power and time as well as UV exposure dosage and time are important factors in the repeatability of the process and need further investigation.

Finally, in the spin-coating step of NOA81, the liquid is dispensed directly from the bottle, and there is a chance that bubbles entrap in the liquid. In that case, the visible bubbles can be burst open carefully with a sharp tip. Smaller air bubbles may remain in the material but will not be observed in the microscopy technique as detrimental as demonstrated in Fig. 7 (Sec. III C), since the focus height in the culture is not in the NOA81 nanogroove material or directly at the exact interface between NOA81 surface and the cells themselves when utilized in 3D brain-on-chip cultures.

Resting time of NOA81 in the PDMS mold prior to UV exposure could also positively affect the filling of narrow grooves by the liquid adhesive and enhance the pattern fidelity for such features. Placing the PDMS mold with NOA81 on top in a vacuum chamber could aid removing any microbubbles (if there are any), and even help for a better filling of the grooves; however, whether a vacuum environment influences the properties of NOA81 needs further investigation too.

C. Optical transparency of microtransfer molded NOA81 nanogrooves

The optical transparency of the film in imaging applications is determined by the thickness, uniformity, surface quality of interfaces, and pattern fidelity of the microtransferred NOA81 nanogrooves. The thickness and uniformity of the transferred film can be controlled by the parameters in the NOA81 spin-coating process, and specifically by the speed in step (b) of the procedure as given in Sec. II A. To characterize the influence of the spin speed, a spin curve is taken, and the resulting film thickness was measured by a profilometer, for which the data are depicted in Fig. 6. The measurements are performed on the NOA81 thin films spin-coated with 6000–12 000 rpm with an interval of 2000 rpm ($n = 3$). The results show that thin films of less than $2 \mu\text{m}$ can be achieved with a speed of 10 000 rpm at the given NOA81 viscosity as provided directly by the supplier's data sheet (300 cps at 25°C). We aimed to achieve the thinnest NOA81 film possible at this

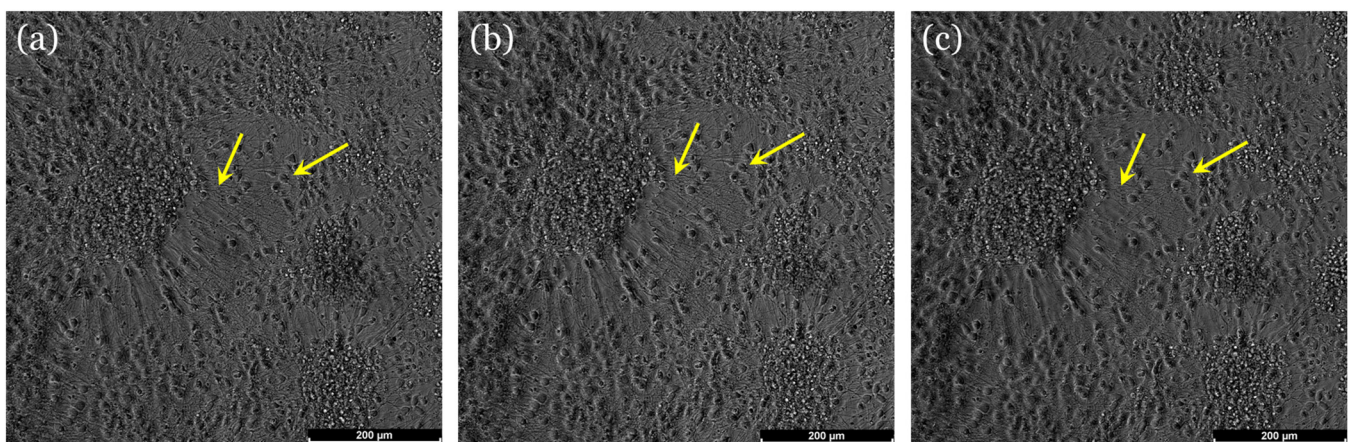


FIG. 7. Comparing the images of differentiated neuronal stem cells with and without NOA81 in the optical path underneath the culture dish: on glass only (a), on flat NOA81 substrate (b), and on NOA81 nanogrooves (c). The arrows highlight the locations of similar neurites and neuronal cell bodies in the images.

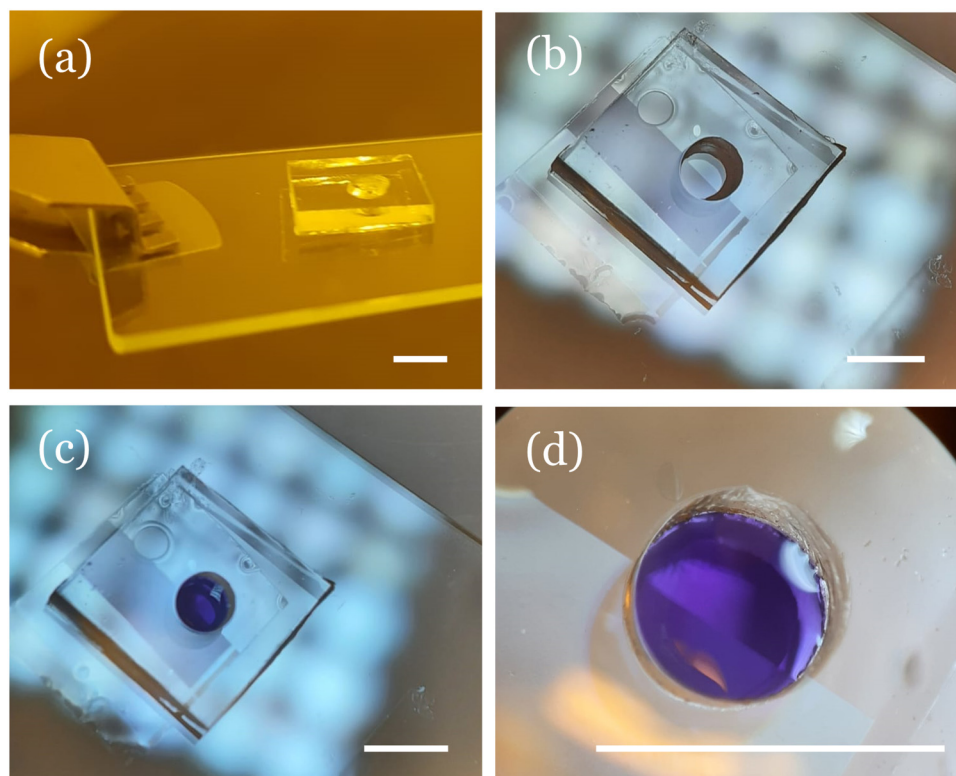


FIG. 8. Microphysiological system on glass slide (a) consisting of a 3-mm diameter single PDMS well bonded half to NOA81 nanogrooves and half to a flat NOA81 surface side-by-side (b). The dye is placed inside the well to verify the bonding properties of the device (c) and (d). Scale bars: 5 mm for (a)–(d).

given NOA81 viscosity to show the potential of fabricating and handling such thin nanogrooved films in microtransfer molding as well as demonstrate its optical performance. Therefore, the maximum spin-coating speed was selected. The highest speed available in the spin-coater in our lab is 12 000 rpm; hence, the samples for the measurements were prepared with this condition, which yielded a film thickness of $1.6 \pm 0.1 \mu\text{m}$.

To evaluate the optical transparency of NOA81 films, Fig. 7 illustrates, by example, viewing cells in a culture. A culture dish with cells was placed on a clean coverslip as a control experiment [Fig. 7(a)], on flat NOA81 films [Fig. 7(b)], and nanogrooved NOA81 films [Fig. 7(c)], respectively. Comparing these three images by observing neurites and cell bodies (arrows in Fig. 7), it becomes obvious that the NOA81 layer (either patterned or not) does not obstruct the optical transparency. Hence, μTm of NOA81 nanogroove films can also be further implemented in devices, wherein this level of detail in bottom-up microscopy is important, e.g., in microsieves for brain-on-chip applications.⁶ Microtransfer molding of NOA81 can be used, for example, to fabricate either nanogroove or flat bottom microwell plates to study the influence of these anisotropic patterns on cells further. The microwell fabrication is described in Sec. III D.

D. Assembly of nanogrooves with PDMS parts for microfluidic applications

To incorporate nanogroove substrates in cell culture experiments, appropriate devices need to be fabricated. As described in

Sec. II C, a PDMS part with a single 3-mm diameter well is bonded on NOA81 nanogrooves as a proof-of-concept [Fig. 8(a)]. In this device, different regions of nanogrooves and flat substrates can be presented to the cultures inside a well-plate format to examine the influence of nanogroove-cell interactions [Fig. 8(b)]. The conventional way of bonding PDMS to glass or PDMS parts that includes surface activation using plasma does not provide a permanent and leakage-free bond between NOA81 surfaces and PDMS components. Therefore, we used an additional amount of NOA81 as a bonding agent to fabricate this assembly. To verify whether the bonding between these two components is well established, we placed a dye inside the well [Fig. 8(c)] and we observed that it remained in the well without leakage [Fig. 8(d)].

IV. SUMMARY AND CONCLUSIONS

Nanogrooves are established to show a beneficial influence on neuronal cell differentiation and alignment of outgrowths. Hence, we demonstrated a fabrication method for such structures using NOA81, which is a biocompatible⁶ optical adhesive. SEM images show that qualitative nanogrooves have been transferred to some extent. By AFM, we then demonstrated a quantitative proof of the successful microtransfer molding of the pattern onto an acceptor substrate by providing a well-defined thin film of NOA81 ($1.6 \mu\text{m}$ thickness) using spin-coating onto a plasma treated PDMS working mold. Cross-sectional SEM studies would certainly add value to the critical characterization of the structures. Unfortunately, these were not yet achieved in this polymeric material, which is very sensitive

to the heat generated in the focused ion beam (FIB) cross sectional-cut preparation steps. We have also shown that a single PDMS working mold can be used for at least six consecutive pattern transfers. We have further demonstrated the fabrication of NOA81 nanogrooves implemented in a well-plate format made from PDMS. In this arrangement, the bottom of the well is covered half by nanogroove and half by a flat NOA81 surface. Microtransfer molding of NOA81 nanogroove thin films therefore provides a feasible route to facilitate biological experiments that aim to introduce topographical cell guidance or neurite alignment.

ACKNOWLEDGMENTS

This work has received funding from the European Union's Horizon 2020 Research And Innovation Programme H2020-FETPROACT-2018-01 under Grant Agreement No. 824070 and the collaboration project Nano+, which is a co-funded project by the PPP Allowance made available by Health~Holland, Top Sector Life Sciences & Health, to stimulate public-private partnerships, under Grant Agreement No. LSHM19006. We thank Sijia Xie for the fabrication of the original COC master for the soft lithography utilizing J-FIL and thermal nanoimprint lithography at the University of Twente. Moreover, we thank the members of the Microfab/lab at the Eindhoven University of Technology for their experimental support, and specifically Alex J. Bastiaens for training on the soft lithography technique using the COC molds and Yagmur Demircan Yalcin for assisting in the microscopy and imaging of the differentiated neuronal stem cells.

DATA AVAILABILITY

The data that support the findings of this study are available from the corresponding author upon reasonable request.

REFERENCES

- ¹Norland Products Inc., Norland Optical Adhesive 81, see <http://www.norlandprod.com/adhesives/NOA81.html> (accessed 3 August 2021).
- ²D. Bartolo, G. Degré, P. Nghe, and V. Studer, *Lab Chip* **8**, 274 (2008).
- ³P. Wägli, A. Homsy, and N. F. De Rooij, *Sens. Actuators B* **156**, 994 (2011).
- ⁴S. Rezvani, N. Shi, T. M. Squires, and C. F. Schmidt, *J. Phys. D: Appl. Phys.* **51**, 045403 (2018).
- ⁵R. Li *et al.*, *J. Chromatogr. Sci.* **54**, 523 (2016).
- ⁶E. Moonen, R. Luttge, and J. P. Frimat, *Microelectron. Eng.* **197**, 1 (2018).
- ⁷R. Sabahi-Kaviani and R. Luttge, *Micromachines* **12**, 1 (2021).
- ⁸C. Forro, D. Caron, G. N. Angotzi, V. Gallo, L. Berdondini, F. Santoro, G. Palazzolo, and G. Panuccio, *Micromachines* **12**, 124 (2021).
- ⁹T. Osaki, Y. Shin, V. Sivathanu, M. Campisi, and R. D. Kamm, *Adv. Healthcare Mater.* **7**, 1700489 (2018).
- ¹⁰P. Nikolakopoulou, R. Rauti, B. M. Maoz, and A. Herland, *Brain* **143**, 3181 (2020).
- ¹¹M. Kitsara, D. Kontziampasis, O. Agbulut, and Y. Chen, *Microelectron. Eng.* **203–204**, 44 (2019).
- ¹²J. Deng, W. Wei, Z. Chen, B. Lin, W. Zhao, Y. Luo, and X. Zhang, *Micromachines* **10**, 1 (2019).

- ¹³N. Azizipour, R. Avazpour, D. H. Rosenzweig, M. Sawan, and A. Aji, *Micromachines* **11**, 599 (2020).
- ¹⁴M. A. Signore, C. De Pascali, L. Giampetruzzi, P. A. Sciliano, and L. Francioso, *Sens. Bio-Sens. Res.* **33**, 100443 (2021).
- ¹⁵M. Zhang, C. Xu, L. Jiang, and J. Qin, *Toxicol. Res.* **7**, 1048 (2018).
- ¹⁶P. M. Holloway, S. Willaime-Morawek, R. Siow, M. Barber, R. M. Owens, A. D. Sharma, W. Rowan, E. Hill, and M. Zagnoni, *J. Neurosci. Res.* **99**, 1276 (2021).
- ¹⁷J. Frimat and R. Luttge, *Front. Bioeng. Biotechnol.* **7**, 100 (2019).
- ¹⁸T. Osaki, V. Sivathanu, and R. D. Kamm, *Sci. Rep.* **8**, 5168 (2018).
- ¹⁹A. J. Bastiaens, S. Xie, D. A. M. Mustafa, J. Frimat, J. M. J. Den Toonder, and R. Luttge, *Front. Cell. Neurosci.* **12**, 415 (2018).
- ²⁰A. Bastiaens, R. Sabahi-Kaviani, and R. Luttge, *Front. Neurosci.* **14**, 666 (2020).
- ²¹S. Xie, B. Schurink, F. Wolbers, R. Luttge, and G. Hassink, *J. Vac. Sci. Technol. B* **32**, 06FD03 (2014).
- ²²A. Bastiaens, J. Frimat, T. Van Nunen, and R. Luttge, *J. Vac. Sci. Technol. B* **37**, 061802 (2019).
- ²³M. Arvidsson, L. Ringstad, L. Skedung, K. Duvefelt, and M. W. Rutland, *Biotribology* **11**, 92 (2017).
- ²⁴Z. Wang, A. A. Volinsky, and N. D. Gallant, *J. Appl. Polym. Sci.* **131**, 41029 (2014).
- ²⁵C. Wang and J. Park, *Micro Nano Syst. Lett.* **8**, 1 (2020).
- ²⁶N. Sandström, R. Z. Shafagh, A. Vastesson, C. F. Carlborg, W. Van Der Wijngaart, and T. Haraldsson, *J. Micromech. Microeng.* **25**, 075002 (2015).
- ²⁷Z. Yan, X. Huang, and C. Yang, *Microfluid. Nanofluid.* **21**, 1 (2017).
- ²⁸X. Zhao, Y. Xia, and G. M. Whitesides, *J. Mater. Chem.* **7**, 1069 (1997).
- ²⁹S. Xie, "Brain-on-a-chip integrated neuronal networks," Ph.D. thesis (University of Twente, 2016).
- ³⁰S. Xie and R. Luttge, *Microelectron. Eng.* **124**, 30 (2014).
- ³¹D. Nečas and P. Klapetek, *Cent. Eur. J. Phys.* **10**, 181 (2012).
- ³²A. J. Bastiaens, S. Xie, and R. Luttge, *J. Vac. Sci. Technol. B* **36**, 06J801 (2018).
- ³³S. Chakraborty, *Microfluidics and Microscale Transport Processes* (CRC, Boca Raton, FL, 2012).
- ³⁴J. Zhou, A. V. Ellis, and N. H. Voelcker, *Electrophoresis* **31**, 2 (2010).
- ³⁵M. Kitsara and J. Ducreé, *J. Micromech. Microeng.* **23**, 033001 (2013).
- ³⁶H. Hocheng, C. M. Chen, Y. C. Chou, and C. H. Lin, *Microsyst. Technol.* **16**, 423 (2010).
- ³⁷R. Seghir and S. Arscott, *Sens. Actuators A* **230**, 33 (2015).
- ³⁸A. Mata, A. J. Fleischman, and S. Roy, *Biomed. Microdevices* **7**, 281 (2005).
- ³⁹Z. Brounstein, J. Zhao, D. Geller, N. Gupta, and A. Labouriau, *Polymers* **13**, 3125 (2021).
- ⁴⁰J. Kim, M. K. Chaudhury, M. J. Owen, and T. Orbeck, *J. Colloid Interface Sci.* **244**, 200 (2001).
- ⁴¹D. T. Eddington, J. P. Puccinelli, and D. J. Beebe, *Sens. Actuators B* **114**, 170 (2006).
- ⁴²See the supplementary material at <https://www.scitation.org/doi/suppl/10.1116/6.0001333> for details of the AFM measurements of all six consecutive NOA81 nanogroove microtransfers using the same PDMS working mold. This material also contains SEM images of tilted microtransfer molded NOA81 nanogrooves to present a side view of the sidewalls of the nanogrooves. Furthermore, the details about using optical diffraction technique to characterize the periodicity of our PDMS nanogrooves patterns of the PDMS working mold as well as the resulting transferred NOA81 nanogrooves are included in the supplementary material.